



## Production of CO-free H<sub>2</sub> from formic acid. A comparative study of the catalytic behavior of Pt metals on a carbon support

F. Solymosi\*, Á. Koós, N. Liliom, I. Ugrai

Reaction Kinetics Research Group, Chemical Research Centre of the Hungarian Academy of Sciences, Department of Physical Chemistry and Materials Science, University of Szeged, P.O. Box 168, H-6701 Szeged, Hungary

### ARTICLE INFO

#### Article history:

Received 17 December 2010  
Revised 21 January 2011  
Accepted 21 January 2011  
Available online 24 February 2011

#### Keywords:

Formic acid decomposition  
Reforming of formic acid  
Production of CO-free H<sub>2</sub>  
Pt metals  
Carbon support

### ABSTRACT

The vapor-phase decomposition of formic acid was investigated over Pt metals supported on inert carbon Norit with the aim of producing CO-free H<sub>2</sub>. FTIR spectroscopic studies revealed that formic acid dissociated on Pt metals at 220–240 K, but the formate species formed was stable only below 300–350 K. Decomposition of formic acid started at and above 350 K on all catalysts and was complete at 473–523 K. Kinetic studies on Pt/Norit demonstrated that the decomposition was a zero-order process with an activation energy of 70.7 kJ/mol. Although dehydrogenation was the predominant process at lower temperatures, CO-free H<sub>2</sub> was not produced on any catalyst. The highest selectivity of 98.3–99% for H<sub>2</sub> formation was attained on Ir/Norit. For all catalysts, the selectivity was improved considerably by the addition of water to formic acid. The production of CO-free H<sub>2</sub> was achieved only on supported Ir at 383–473 K. Similarly, as regards the H<sub>2</sub> yield the outstanding catalyst was Ir/Norit, followed by Pt/Norit.

© 2011 Elsevier Inc. All rights reserved.

### 1. Introduction

Great efforts have been made during the last decade to develop an efficient catalytic process for the production of H<sub>2</sub> [1–3]. The most frequently used source is an alcohol, and particularly ethyl alcohol, but elimination of large amount of CO and C<sub>x</sub>H<sub>y</sub>O compounds formed causes great difficulty, not to mention the poisoning effect of acetate [4–6]. Unfortunately, the decomposition of CH<sub>4</sub> and other hydrocarbons is less applicable due to carbon deposition and early deactivation of the catalyst [7–9]. In the field of heterogeneous catalysis, formic acid as a source of H<sub>2</sub> has received attention only recently [10–13], although it has been considered as a possible basic material for the production of H<sub>2</sub> for fuel cells [14,15]. Note that formic acid may be obtained from biomass conversion. The decomposition of formic acid was widely used as a model reaction in the 1950s and 1960s to test the roles of the electronic properties of metals, alloys and pure and doped oxides in heterogeneous catalysis [16–23]. It was demonstrated that the electronic properties of both the metals and the oxides play an important part in the catalysis of formic acid decomposition [15–23]. The study of this reaction provided the first convincing evidence of the importance of the electronic interactions between Ni and semiconducting supports (TiO<sub>2</sub>, NiO and Cr<sub>2</sub>O<sub>3</sub>) in carrier effect [19,20].

Renewed interest in the catalytic chemistry of formic acid [24–27] resulted from the observations that formate species are important reaction intermediates in several catalytic processes, e.g. CH<sub>3</sub>OH synthesis [28] and reforming [29], the water–gas shift reaction [30] and the hydrogenation of CO<sub>2</sub> [31–35] and CO [36,37]. This also initiated great interest in the study of the interactions of formic acid with metal single crystals on an atomic scale [38–40]. In addition, great number of papers dealt with the decomposition of formic acid in solution using various metal complexes. The results are well summarized in some excellent papers and reviews [41–44].

We recently found that Mo<sub>2</sub>C prepared by the reaction of MoO<sub>3</sub> with multiwall carbon and carbon Norit, which exhibited high activities in the reactions of C<sub>2</sub>H<sub>5</sub>OH, CH<sub>3</sub>OH and (CH<sub>3</sub>)<sub>2</sub>O [45], is also an efficient catalyst for the decomposition and reforming of formic acid [12]. At certain temperatures, CO-free H<sub>2</sub> can be produced in a yield of 99–100%. In the present paper, we examine the catalytic performances of Pt metals, mainly supported on carbon Norit, in the reactions of formic acid, with the aim of identifying the most active metal and establishing experimental conditions under which H<sub>2</sub> can be produced in high yield and virtually free of CO.

### 2. Experimental

Carbon Norit (Alfa Aesar, ROW 0.8 mm pellets, Steam activated) was used as a support, which was purified by treatment with HCl (10%) for 12 h at room temperature. Afterward it was washed to have a Cl-free sample. After this treatment, the metal impurities,

\* Corresponding author. Fax: +36 62 544 106.

E-mail address: [fsolym@chem.u-szeged.hu](mailto:fsolym@chem.u-szeged.hu) (F. Solymosi).

mainly Fe, determined by the ICP-AES method, amounted to less than 0.002%. The surface area of the purified sample is 859 m<sup>2</sup>/g. The supported catalysts were prepared by impregnating the carbon Norit with solutions of metal compounds to yield a nominal 2 wt% metal. The following salts of Pt metals were used: H<sub>2</sub>PtCl<sub>5</sub>·6H<sub>2</sub>O, PdCl<sub>2</sub>, RhCl<sub>3</sub>·3H<sub>2</sub>O, H<sub>2</sub>IrCl<sub>6</sub> and RuCl<sub>3</sub>·3H<sub>2</sub>O. The impregnated powders were dried at 383 K. The fragments of catalyst pellets were oxidized at 673 K and reduced at 673 K for 1 h *in situ*. In a certain case SiO<sub>2</sub> (CAB-O-SIL; 198 m<sup>2</sup>/g) and Al<sub>2</sub>O<sub>3</sub> (Degussa, P110, 100 m<sup>2</sup>/g) were also used as a support. HCOOH was the product of BDH, with a purity of 99.5%. Other gases were of commercial purity (Linde).

The dispersion of metals was determined by the adsorption of H<sub>2</sub> at room temperature. Thermal desorption measurements (TPD) were carried out in the catalytic reactor. The catalysts were treated with HCOOH/Ar containing ~6% HCOOH at ~300 K for 60 min, and flushed with Ar for 30 min. The TPD were carried out in Ar flow (20 ml/min) with ramp at 2 K/min from 300 K to ~700 K. Desorbing products were analyzed by gas chromatography. Fourier Transformed Infra Red (FTIR) spectra were recorded with a BioRad FTS-155 spectrometer with a wavenumber accuracy of ±4 cm<sup>-1</sup>. Catalytic reactions were carried out at a pressure of 1 atm in a fixed-bed, continuous flow reactor consisting of a quartz tube (8 mm id) connected to a capillary tube [12]. The flow rate was 40 ml/min. The carrier gas was Ar, which was bubbled through the formic acid at room temperature: its content was ~5–6.0%. In general, 0.3 g of loosely compressed catalyst sample was used. The reaction products were analyzed with a HP 4890 gas chromatograph equipped with PORAPAQ Q+S and 30-m long HP-PLOT Al<sub>2</sub>O<sub>3</sub> column. The conversion of formic acid was determined by taking into account the amount consumed. The selectivity of hydrogen was calculated from the ratio of CO<sub>2</sub> concentration to the sum of CO<sub>2</sub> + CO. Multiplying this value with the conversion gave the hydrogen yield.

### 3. Results

#### 3.1. Infrared spectroscopic measurements

As Pt metals on a carbon support are not transparent, IR measurements were first performed with silica-supported metals.

Fig. 1A depicts the IR spectra of formic acid adsorbed on Ir/SiO<sub>2</sub> at ~200 K and heated to different temperatures under continuous degassing. In the C–H stretching region, absorption bands were observed at 2942, 2920 and 2847 cm<sup>-1</sup>, with intensities which gradually attenuated as the temperature was raised. In the low-frequency range, a very intense spectral feature appeared at 1722 cm<sup>-1</sup>, and less intense one at 1391 cm<sup>-1</sup>. At around 225 K, weak new bands started to develop at 1586, 1369 and 1270 cm<sup>-1</sup>. The intensity of the 1586 cm<sup>-1</sup> increased up to 253–273 K, but then attenuated, and it disappeared at around 290–300 K. The 1722 cm<sup>-1</sup> band also underwent attenuation, but remained detectable up to 300 K. Analogous features were found on Rh/SiO<sub>2</sub> (Fig. 1B). In this case the band at 1590 cm<sup>-1</sup> was somewhat more stable and could be detected even at ~473 K. Similar spectral features were likewise observed on the other SiO<sub>2</sub>-supported metals. The position of the absorption bands is given in Table 1.

The interaction of formic acid with Ir/Al<sub>2</sub>O<sub>3</sub> resulted in a different picture. In this case, it was not necessary to perform low-temperature experiments, as the adsorption of formic acid even at 300 K produced very strong bands at 1597, 1394 and 1381 cm<sup>-1</sup>, and a less intense one at 1714 cm<sup>-1</sup>. The latter gradually attenuated at higher temperature and disappeared at 273–300 K. In contrast with the results observed on SiO<sub>2</sub>-supported metals, the 1597 cm<sup>-1</sup> band exhibited high thermal stability: it was eliminated only above 573 K (Fig. 2). The adsorption of formic acid on

**Table 1**

Vibrational frequencies (in cm<sup>-1</sup>) observed following the adsorption of HCOOH and their assignment.

Assignment	Ir/SiO <sub>2</sub>	Rh/SiO <sub>2</sub>	Ir/Al <sub>2</sub> O <sub>3</sub>
ν(CH)	2942	2944	2933
ν(CH)	2920	2917	2913
ν(CH) (formate)	2847	2863	
ν(CO) (formic acid)	1722	1723	1714
ν <sub>a</sub> (OCO)	1586	1590	1597
ν(OCO) (formic acid and formate)	1391	1375	1394
ν <sub>s</sub> (OCO)	1369	1310	1381
ν(CO)	1270		1326
ν(CH)			1079

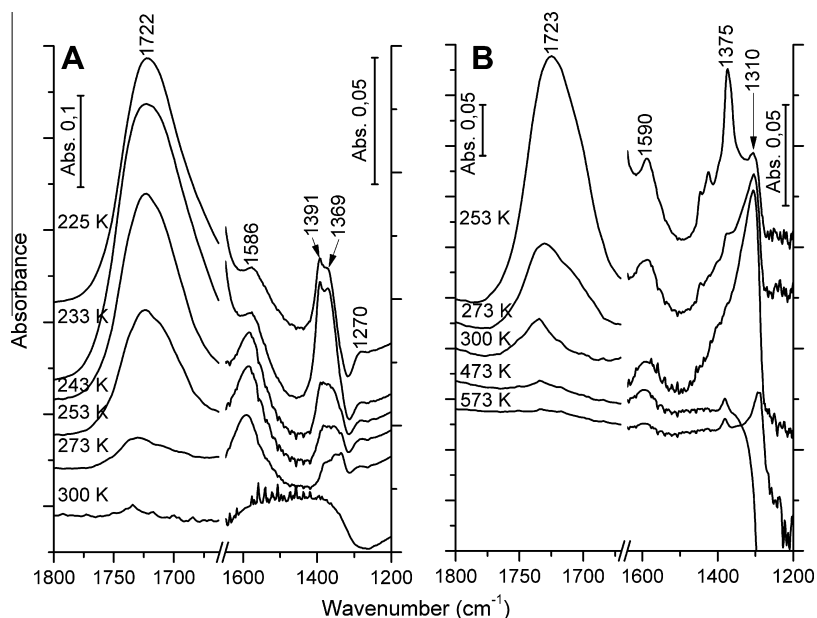


**Fig. 1.** FTIR spectra of Ir/Norit (A) and Rh/Norit (B) following the adsorption of HCOOH at ~200 K and after subsequent degassing at different temperatures.

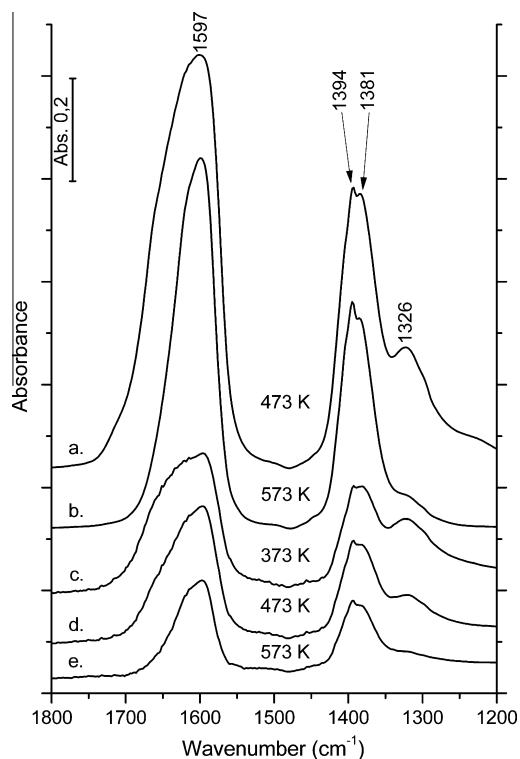


**Fig. 2.** FTIR spectra of  $\text{Al}_2\text{O}_3$  (a, b) and  $\text{Ir}/\text{Al}_2\text{O}_3$  (c–e) following the adsorption of  $\text{HCOOH}$  at 300 K and after subsequent degassing at different temperatures.

pure  $\text{Al}_2\text{O}_3$  produced exactly the same spectral features, with the difference that the  $1597\text{ cm}^{-1}$  band was more stable. Note that in addition to the above absorption bands weak signals were also identified at  $2040\text{--}2050\text{ cm}^{-1}$  for Ir samples and at  $2060\text{ cm}^{-1}$  for  $\text{Rh}/\text{SiO}_2$ .

### 3.2. Thermal desorption measurements

TPD spectra for various products after the adsorption of formic acid on different samples at  $\sim 300\text{ K}$  are presented in Fig. 3. The weakly adsorbed formic acid was released from every sample immediately above 300 K. Desorption of other compounds from

$\text{Ir}/\text{Norit}$  is characterized by the following peak temperatures:  $\text{H}_2$  ( $T_p = 400\text{ K}$ ) and  $\text{CO}$  ( $T_p = 375\text{ K}$ ). From the pure Norit support, we registered the desorption of formic acid with  $T_p \approx 315\text{ K}$ , without the formation of  $\text{H}_2$ ,  $\text{CO}$  or  $\text{CO}_2$ . In the case of  $\text{Ir}/\text{SiO}_2$  only the desorption of a very small amount of  $\text{H}_2$  was observed at  $T_p \sim 430\text{ K}$ . From  $\text{Ir}/\text{Al}_2\text{O}_3$ , larger amounts of  $\text{H}_2$  and  $\text{CO}_2$  with  $T_p = 478\text{ K}$ , and a smaller quantity of  $\text{CO}$  with  $T_p = 500\text{ K}$  were released.

### 3.3. Catalytic measurements

#### 3.3.1. Decomposition of formic acid

Fig. 4 illustrates the conversion in the decomposition of formic acid and the selectivity of  $\text{H}_2$  formation on the carbon-supported metals as a function of temperature. The reaction began at and above 350 K on all samples and was complete at 473–523 K. The main process was the dehydrogenation of formic acid to  $\text{H}_2$  and  $\text{CO}_2$ .  $\text{CO}$  was formed in only 2–7% at lower temperatures, but its amount gradually increased at higher temperatures.

As concerns the catalytic behavior of the Pt metals, the decomposition occurred to a great extent on  $\text{Ir}/\text{Norit}$ . The selectivity for  $\text{H}_2$  production was 98–99% at 423–523 K, which diminished to  $\sim 93\%$  at 623 K. The decomposition rate was lower on  $\text{Pt}/\text{Norit}$ . In this case, the selectivity for  $\text{H}_2$  at 423–473 K was 98–99%, which decreased markedly at higher temperatures. Lower conversions were observed on  $\text{Rh}/\text{Norit}$ . The selectivity for  $\text{H}_2$  formation was  $\sim 91.8\%$  at 423 K, when the conversion was only  $\sim 40\%$ , and the selectivity was only 78.5% at 623 K.  $\text{Pd}/\text{Norit}$  exhibited less activity: total conversion was achieved only at 523 K. The selectivity for  $\text{H}_2$ , 95.8% at 423 K, decreased by only  $\sim 5\%$  up to 623 K. The decomposition occurred at the lowest rate on  $\text{Ru}/\text{Norit}$  with a  $\text{H}_2$  selectivity of 97.2% at 423 K at a conversion of  $\sim 22\%$ . The selectivity decreased to 82% at 623 K. After determination of the temperature dependence of the decomposition of formic acid, we followed the reaction in time on stream at 573 and 623 K for 10–12 h. No or only very slight changes were experienced in the conversion and in the product distribution on any catalyst. Some important data for the decomposition of formic acid on various metals are presented in Table 2.

In order to establish what adsorbed species exist on the surface under dynamic conditions, we performed FTIR spectroscopic studies *in situ* during the catalytic reaction in a flow of a gaseous

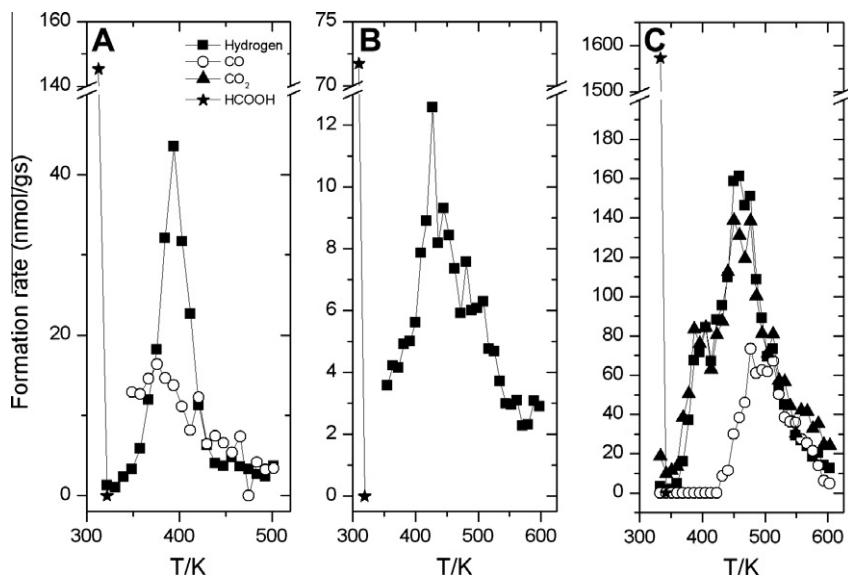


**Fig. 3.** TPD spectra following the adsorption of  $\text{HCOOH}$  on  $\text{Ir}/\text{Norit}$  (A),  $\text{Ir}/\text{SiO}_2$  (B) and  $\text{Ir}/\text{Al}_2\text{O}_3$  (C) at 300 K.

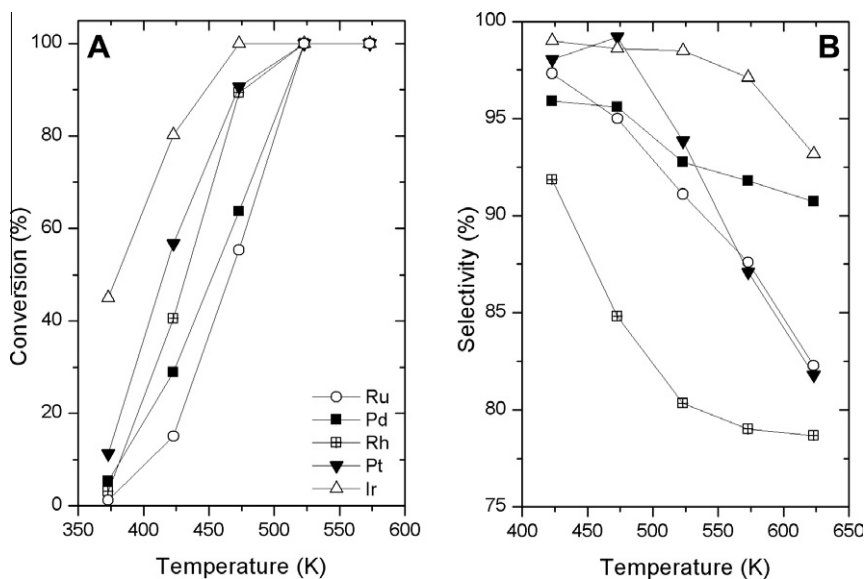


Fig. 4. Conversion of formic acid (A) and the selectivity of H<sub>2</sub> formation (B) on Pt metals supported by carbon Norit as a function of temperatures.

Table 2

Some characteristic data for the decomposition of formic acid on Norit supported Pt metals.

Catalyst	Dispersion (%)	Work function of the metals (eV) [46]	$N_{\text{H}_2}$ ( $\times 10^2$ ) at 373 K	$N_{\text{H}_2}$ ( $\times 10^2$ ) at 423 K	423 K		473 K	
					H <sub>2</sub> selectivity (%)	H <sub>2</sub> yield (%)	H <sub>2</sub> selectivity (%)	H <sub>2</sub> yield (%)
Ir	26.1	5.76	9.6	41.2	99.0	79.2	98.3	98.3
Pt	23.5	5.70	6.4	37.8	98.0	55.6	99.1	89.8
Pd	8.6	5.12	4.4	36.3	95.1	27.7	95.5	60.8
Ru	5.6	4.71	1.3	25.3	97.3	15.2	94.9	52.5
Rh	24.3	4.98	0.9	12.8	91.8	37.2	84.8	75.7

$N_{\text{H}_2}$  = turnover numbers given by:  $\left(\frac{\text{Molecules formed}}{\text{Metal site (s)}}\right)$ .

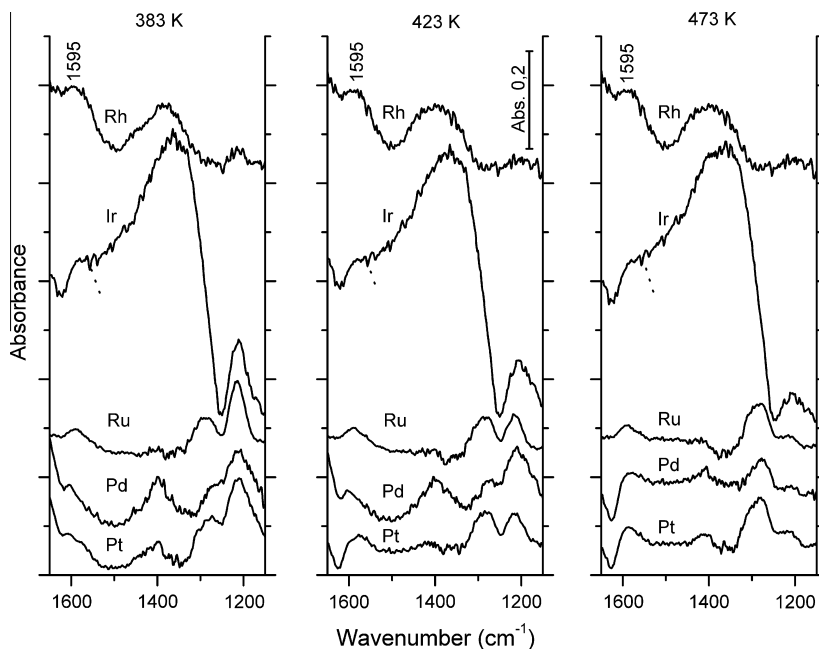


Fig. 5. *In situ* IR spectra registered on silica supported Pt metals during the decomposition of formic acid at different temperatures.

mixture of HCOOH + Ar. This study was carried out in the DRIFT cell. Beside the intense absorption band due to formic acid at 1720–1730 cm<sup>-1</sup>, weak spectral features appeared at 1595, 1395–1400 and ~1200 cm<sup>-1</sup> for all samples. With the rise of the

reaction temperature their intensities remained practically unaltered. In the CO stretching region, weak absorption bands were also detected at 2030–2050 cm<sup>-1</sup>. When the stream of HCOOH + Ar was changed to pure Ar, all the absorption bands disappeared at

once, with the exception of that due to CO. Selected regions of IR spectra are displayed in Fig. 5.

On the 2% Pt/Norit catalyst, we performed kinetic measurements in the temperature range 380–425 K. The partial pressure of formic acid was varied, with the total flow rate kept at 40 ml min<sup>-1</sup> by the addition of Ar ballast to the system. The decomposition of formic acid under these conditions followed zero-order kinetics. The Arrhenius plots yielded 70.7 kJ/mol ± 3 kJ/mol for the activation energy of the formation of H<sub>2</sub>. This value is consistent with previous data, 75 kJ/mol on Rh/Al<sub>2</sub>O<sub>3</sub> [25], 72 kJ/mol on Pt/Al<sub>2</sub>O<sub>3</sub> [10] and 67 kJ/mol on Pd/C [11].

### 3.3.2. Reforming of formic acid

The addition of water to the formic acid (HCOOH:H<sub>2</sub>O = 1:1) influenced the conversion of formic acid at different temperatures only slightly, but affected the product distribution and enhanced the selectivity of H<sub>2</sub> formation to various extents. As dehydrogenation predominated at lower temperatures, the reforming of formic acid was followed in time on stream at 383, 423 and 473 K. The selectivity data determined for various catalysts demonstrated that, apart from minor fluctuations, little change occurred in time on stream (Fig. 6). CO-free H<sub>2</sub> was obtained on 2% Ir/Norit at 383 K. S<sub>H<sub>2</sub></sub> decreased to ~99.5% at 423 and 473 K. On 5% Ir/Norit, S<sub>H<sub>2</sub></sub> remained 100% in the temperature range 383–473 K. Very high values of 99.5–99.2% were measured for Pd/Norit and Pt/Norit at 383 K, when that for Ru/Norit was ~98%, which diminished to 97.5% and 95.0% at 423 and 473 K, respectively. Rh/Norit exhibited different behaviors as the highest selectivity, 96.0–97.0%, was manifested at 423–473 K and the lowest at 383 K. This feature was reproducible. In order to obtain more information on the efficiency of the catalyst in the generation of H<sub>2</sub> we calculated the yield of H<sub>2</sub> formation. The results on various samples are to be seen in Table 3.

**Table 3**

Some characteristic data for production of H<sub>2</sub> in steam reforming of HCOOH over supported Pt metals.

Catalyst	Temp. (K)	Conv. (%)	H <sub>2</sub> sel. (%)	H <sub>2</sub> yield
2.0% Ir/Norit	383	50	100	50.0
	423	88	99.5	87.5
	473	100	99.5	99.5
5% Ir/Norit	383	87	100	87.0
	423	100	100	100
	473	~100	100	100
2% Ir/SiO <sub>2</sub>	383	38	100	38.0
	423	48	99.0	47.5
	473	95	98.0	93.1
2% Pt/Norit	383	25	99.2	24.8
	423	52	99.0	51.4
	473	100	98.6	98.6
2% Rh/Norit	383	15	~86.0	12.9
	423	26	97.0	25.2
	473	100	97.0	97.0
2% Pd/Norit	383	15	99.5	14.9
	423	31	98.7	30.5
	473	95	96.6	91.7
2% Ru/Norit	383	18	98.0	17.6
	423	25	97.5	24.3
	473	66	95.0	62.7

## 4. Discussion

### 4.1. Interaction of HCOOH with Pt metals

At 200–250 K, on Ir/SiO<sub>2</sub>, all the absorption bands characteristic of molecularly adsorbed formic acid appeared in the IR spectrum (Fig. 1). The assignments of the bands are shown in Table 1. When the sample was heated, the intensities of all the bands gradually

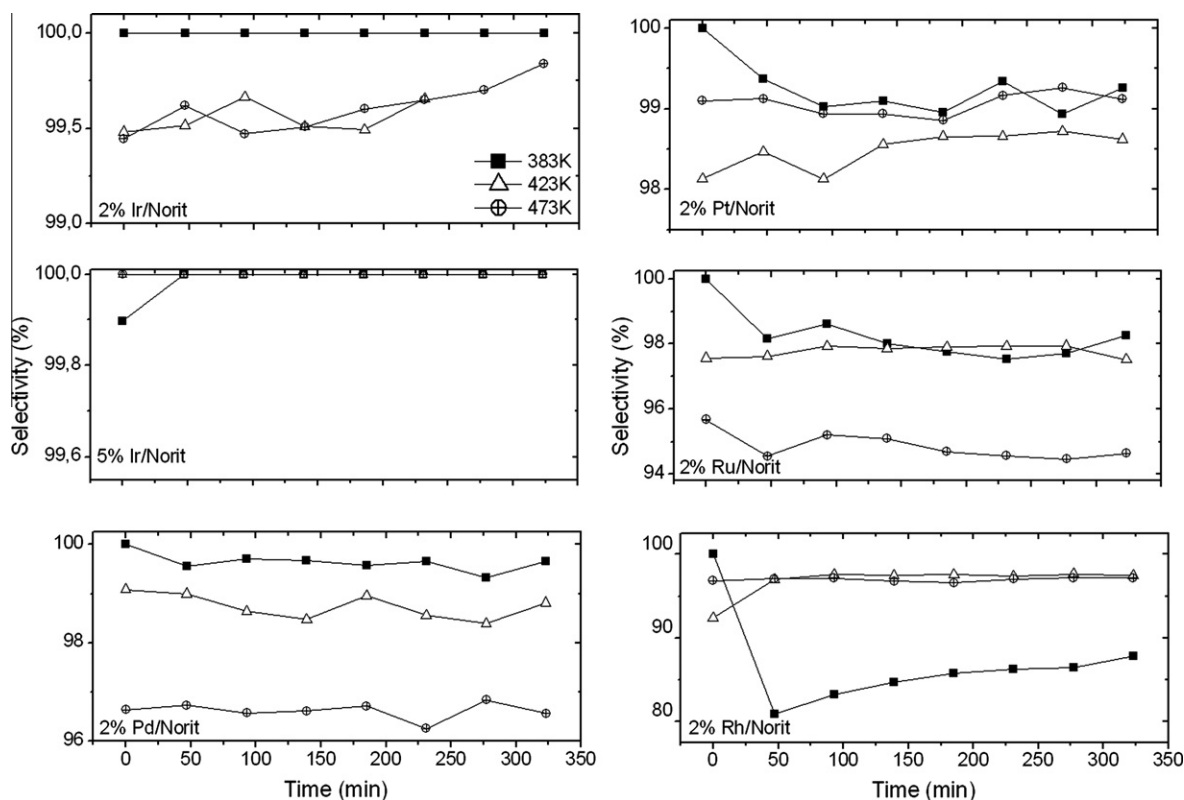


**Fig. 6.** Selectivity of hydrogen formation in the reforming of HCOOH on Pt metals supported by carbon Norit at different temperatures (HCOOH:H<sub>2</sub>O = 1:1).

decreased. Besides the most intense band of formic acid at  $1722\text{ cm}^{-1}$  new spectral features were detected at  $1586$  and  $1369\text{ cm}^{-1}$  at and above  $225\text{ K}$ . The appearance of these vibrations strongly suggests the dissociation of formic acid and the formation of formate species, very likely bonded to Ir:



This conclusion is supported by the results on pure  $\text{SiO}_2$ , when this band was missing at both low and high temperatures. This is in harmony with the experience that formic acid does not dissociate to formate on  $\text{SiO}_2$  [21,22,25,47,48]. The absorption bands due to formate, however, were detected only up to  $290\text{--}300\text{ K}$ , indicating the decomposition of formate species on Ir:



In addition to the formate bands, weak absorption peak appeared at  $2040\text{ cm}^{-1}$ , which can be attributed to CO linearly bonded to an Ir<sub>x</sub> cluster [49]. This suggests another route of decomposition of surface formate:



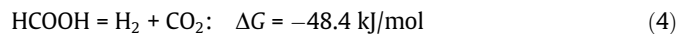
Interestingly, there was no indication of absorption bands at  $\sim 2107$  and  $\sim 2037\text{ cm}^{-1}$  due to the surface dicarbonyl complex  $\text{Ir}^+(\text{CO})_2$ . Similar measurements were carried out on other samples. As shown in Fig. 1B, the adsorption of formic acid on Rh/SiO<sub>2</sub> at  $\sim 200\text{ K}$  produced similar spectral features, but the formate bands were somewhat more stable. In this case, the CO bands developed at  $2060\text{ cm}^{-1}$ . Vibrations due to  $\text{Rh}^+(\text{CO})_2$  at  $2030$  and  $2100\text{ cm}^{-1}$  were again missing. Previous FTIR and STM studies revealed that dicarbonyl complex is formed in the CO-induced oxidative disruption of Rh and Ir nanoparticles [49,50]. The absence of this species is probably due to the presence of H<sub>2</sub>, which hinders the disruption processes [50]. We obtained very similar results on other SiO<sub>2</sub>-supported metals. The stability of the formate bands depended only slightly on the nature of the metals, and the bands were eliminated at  $290\text{--}373\text{ K}$ . The low stability of formate on Pt metals is in harmony with the results obtained on single crystals of these metals by various electron spectroscopic methods [38–40].

A completely different picture was observed for Ir/Al<sub>2</sub>O<sub>3</sub> (Fig. 2). In this case, strong absorption bands due to formate species appeared even following the adsorption of formic acid at  $300\text{ K}$ , and they were detectable up to  $573\text{ K}$ . As the adsorption of formic acid on Al<sub>2</sub>O<sub>3</sub> produced the same IR spectra, it can be concluded that the formate is located not on the Ir, but rather on the Al<sub>2</sub>O<sub>3</sub>. A comparison of the thermal behavior of the formate band at  $1597\text{ cm}^{-1}$  on Ir/Al<sub>2</sub>O<sub>3</sub> and on pure Al<sub>2</sub>O<sub>3</sub> revealed that this species was appreciably more unstable on Ir/Al<sub>2</sub>O<sub>3</sub>. A possible reason is that Ir promotes the decomposition of formate that diffuses to the metal/oxide interface.

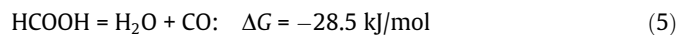
The results of the TPD are in harmony with the IR studies. The desorption of formic acid observed at  $\sim 300\text{ K}$  very likely originates from the formic acid molecularly adsorbed on SiO<sub>2</sub> or carbon Norit supports. The H<sub>2</sub> and a small amount of CO released at higher temperatures are the products of the decomposition of formate at  $\sim 300\text{ K}$ , which remained adsorbed on the metals. As CO<sub>2</sub> is not chemisorbed on Pt metals at  $300\text{ K}$ , no desorption of CO<sub>2</sub> was established by TPD. In harmony with the IR spectroscopic studies, the situation was different for Ir/Al<sub>2</sub>O<sub>3</sub>. Besides H<sub>2</sub> and CO, a large amount of CO<sub>2</sub> also evolved as a result of the decomposition of stable formate on the Al<sub>2</sub>O<sub>3</sub> at higher temperatures.

#### 4.2. Decomposition and reforming of formic acid

Formic acid is a convenient source of H<sub>2</sub>, and its decomposition is the simplest reaction via which to produce H<sub>2</sub>. Only two reaction pathways need to be considered:



and



If the space velocity is high, and the temperature is low enough, the occurrence of secondary reactions can be excluded, such as the hydrogenation of CO<sub>2</sub> to CH<sub>4</sub>, which is well catalyzed by supported Pt metals [31–35]. All the Pt metals are active in the decomposition of formic acid, but with appreciable differences in catalytic efficiency (Fig. 4A). The differences in catalytic behavior show up in the selectivity of H<sub>2</sub> formation, particularly at higher temperatures (Fig. 4B). The conversion data in Fig. 4A indicate the activity sequence Ir > Pt > Rh > Pd > Ru.

A huge number of data initially suggested the importance of the electronic factor in the decomposition of formic acid on different metals and oxides [16–21]. Those catalysts were found to be active which were able to accept electrons from formic acid or its dissociation products. Later, as the role of the electron theory of catalysis declined, however, more emphasis was given to the formation and stability of formate on catalyst surfaces [21–27,47,48]. Those metals were considered to be the best catalysts on which this surface complex was formed easily, but was not very stable. Plots of the rate of decomposition at the same temperature as a function of the heat of formation of the corresponding formate yielded “volcano-shaped” curves [47]. The Pt group proved to be the best of 13 metals, but the activities of the metals were not related to the number of surface metal atoms, so this activity sequence cannot be considered as a reliable one [47]. A more reasonable relationship was presented by Barbeau [40,51], who found a linear correlation between the decomposition temperature of formates on metal single crystals and the heat of formation of the corresponding metal oxides. It is to be pointed out that no data for the reactions of formic acid or formate on Ir catalyst were given in either works [21,22,40,47,48]. Taking into account the dispersity of Norit-supported metals, the specific activities of the metals in terms of turnover frequencies ( $N_{\text{H}_2}$ , rates per surface metal atom) were calculated at  $473\text{ K}$  (Table 2). This gave the following sequence: Ir, Pt, Pd, Ru, Rh. This order is nearly the same as obtained by Barbeau [40] on metal single crystal surfaces. As concerns a possible relationship of these data with the electric properties of the metals, their work functions are also given in Table 2. This shows that the specific activity increases with increase in the work function of the metals, i.e. their ability to accept electrons. This may support the early assumption concerning the role of the electric structure of the metals in the decomposition of formic acid.

The situation is more complex as regards the selectivity of H<sub>2</sub> formation, for its temperature dependence varies with the metal. On most of the catalysts, this parameter decreased significantly as the temperature was raised. It is important to note that pure H<sub>2</sub> was not generated by the decomposition of formic acid on any of the catalysts. The selectivity for H<sub>2</sub> at  $423\text{ K}$  decreased in the sequence Ir, Pt, Ru, Pd, Rh.

Higher selectivities for H<sub>2</sub> measured in the reforming reaction are probably a result of the occurrence of the water–gas shift reaction:



As the primary aim of this study was to generate CO-free H<sub>2</sub>, the formation of even a few tenths of one percent of CO makes the catalyst less attractive and should be avoided. H<sub>2</sub> was produced with 98.0–99.5% selectivity on Norit-supported Pt, Pd and Ru at  $383\text{--}423\text{ K}$ . CO<sub>2</sub> completely free of CO was obtained only on Ir catalyst. Moreover, a H<sub>2</sub> yield of 100% was attained only on the Ir/Norit. Iridium remained a highly selective catalyst at  $383\text{ K}$ , even when it was deposited on a SiO<sub>2</sub> support, though the H<sub>2</sub> yield was much less

than that on Ir/Norit (Table 3). Ojeda and Iglesia [10] have recently shown that the selectivity for hydrogen is close to unity on gold nanoparticles supported on Al<sub>2</sub>O<sub>3</sub>. Ross et al. [11] reported a selectivity of 95–99% on Pd/C catalyst.

As regards the occurrence of the decomposition of formic acid on supported Pt metals, we accept the early proposal that it proceeds through the formation and decomposition of formate species. *In situ* IR spectroscopic studies revealed that formate species exists on the catalyst surfaces during the reaction at 383–473 K (Fig. 5). We assume that the slow step in the decomposition is very likely to be the cleavage of the C–H bond in the adsorbed formate. This step may occur more easily on the metals as compared with rupture of the C–O bond in formate, which may be one of the reasons for the preference of the dehydrogenation of formic acid. The large work function of Ir, i.e. its ability to accept electrons from the substrate, may also contribute to its unequaled activity and selectivity. It may be noted that supported Ir is likewise one of the best catalysts in the decomposition of hydrazine [52].

## 5. Conclusions

- (i) FTIR spectroscopic measurements on SiO<sub>2</sub>-supported Pt metals demonstrated the dissociative adsorption of formic acid at 225–230 K. The formate species formed, however, was detectable only up to 300–373 K. *In situ* IR studies revealed that formate exists on the catalyst surface even during the catalytic reaction at 383–473 K.
- (ii) Pt metals deposited on carbon Norit were found to be effective catalysts in the vapor-phase decomposition of formic acid to generate H<sub>2</sub>, though CO-free H<sub>2</sub> was not obtained by the decomposition on any of the metals. Ir/Norit proved to be the best and the most selective catalyst.
- (iii) The addition of water to the formic acid allowed the production of H<sub>2</sub> completely free of CO on Ir catalysts at 383–423 K.

## Acknowledgment

This work was supported by the grant OTKA under Contact Number K 81517.

## References

- [1] G. Sandstede, T.N. Veziroglu, C. Derive, J. Pottier (Eds.), Proceedings of the Ninth World Hydrogen Energy Conference, Paris, France, 1972, p. 1745.
- [2] A. Haryanto, S. Fernando, N. Murali, S. Adhikari, Energy Fuels 19 (2005) 2098.
- [3] F. Marino, M. Boveri, G. Baronetti, M. Laborde, Int. J. Hydrogen Energy 26 (2001) 665.
- [4] C. Diagne, H. Idriss, A. Kiennemann, Catal. Commun. 3 (2002) 565.
- [5] D.K. Liguras, D.I. Kondarides, X.E. Verykios, Appl. Catal. B Environ. 43 (2003) 345.
- [6] A. Erdöhelyi, J. Raskó, T. Kecskés, M. Tóth, M. Dömök, K. Báán, Catal. Today 116 (2006) 367.
- [7] F. Solymosi, Gy. Kutsán, A. Erdöhelyi, Catal. Lett. 11 (1991) 149.
- [8] M. Belgued, H. Amariglio, P. Pareja, A. Amariglio, J. Sain-Just, Catal. Today 13 (1992) 437.
- [9] T. Koerts, M.J.A.G. Deelen, R.A. van Santen, J. Catal. 138 (1992) 101.
- [10] M. Ojeda, E. Iglesia, Angew. Chem. Int. Ed. 48 (2009) 4800.
- [11] D.A. Bulushev, S. Beloshapkin, J.R.H. Ross, Catal. Today 154 (2010) 7.
- [12] Á. Koós, F. Solymosi, Catal. Lett. 138 (2010) 23.
- [13] X. Zhou, Y. Huang, W. Xing, C. Liu, J. Liao, T. Lu, Chem. Commun. (2008) 3540.
- [14] S. Ma, R. Larsen, R.I. Masel, J. Power Sources 144 (2005) 28, and references therein.
- [15] J.H. Choi, K.J. Jeong, Y. Dong, J. Han, T.H. Lim, J.S. Lee, Y.E. Sung, J. Power Sources 163 (2006) 71, and references therein.
- [16] G.-M. Schwab, Discuss. Faraday Soc. 8 (1950) 166; G. Reinäcker, G. Techel, Z. Anorg. Chem. 304 (1960) 58.
- [17] D.D. Eley, P. Luetic, Trans. Faraday Soc. 53 (1957) 1476.
- [18] Z.G. Szabó, F. Solymosi, Acta Chim. Hung. 25 (1960) 145. 161.
- [19] Z.G. Szabó, F. Solymosi, in: Actes Congr. Intern. Catalyse 2e Paris, 1961, p. 1627.
- [20] F. Solymosi, Catal. Rev. 1 (1968) 233.
- [21] G.C. Bond, Catalysis by Metals, Academic, London, 1962.
- [22] P. Mars, J.J.F. Scholten, P. Zweitering, Adv. Catal. 14 (1963) 35.
- [23] J.M. Trillo, G. Munuera, J.M. Criado, Catal. Rev. 7 (1972) 51, and references therein.
- [24] E. Iglesia, M. Boudart, J. Catal. 81 (1983) 214.
- [25] F. Solymosi, A. Erdöhelyi, J. Catal. 91 (1985) 327.
- [26] D.E. Fein, I.E. Wachs, J. Catal. 210 (2002) 241.
- [27] W.-J. Chun, K. Tomishige, M. Hamakado, Y. Iwasawa, J. Chem. Soc. Faraday Trans. 91 (1995) 4161, and references therein.
- [28] A. Deluzarche, R. Kieffer, A. Muth, Tetrahedron Lett. 18 (1977) 3357.
- [29] G.A. Olah, Á. Molnár, Hydrocarbon Chemistry, Wiley-Interscience, New York, 2003.
- [30] Y. Amenomiya, J. Catal. 57 (1979) 64.
- [31] F. Solymosi, A. Erdöhelyi, T. Bácságyi, J. Catal. 68 (1981) 371.
- [32] F. Solymosi, A. Erdöhelyi, in: Proceedings of the 7th International Congress on Catalysis, Tokyo, 1980, Kodansha/Elsevier, Tokyo/Amsterdam, 1981, p. 1448.
- [33] F. Solymosi, A. Erdöhelyi, M. Kocsis, J. Chem. Soc. Faraday Trans. 1 77 (1981) 1003.
- [34] E. Ramarson, R. Kieffer, A. Kiennemann, J. Chem. Soc. Chem. Commun. (1982) 645.
- [35] A. Deluzarche, J. Cressely, R. Kieffer, J. Chem. Res.-S (1979) 136; A. Deluzarche, J. Cressely, R. Kieffer, J. Chem. Res.-M (1979) 1656.
- [36] R.A. Dalla Betta, M. Shelef, J. Catal. 49 (1977) 383.
- [37] F. Solymosi, I. Tombácz, M. Kocsis, J. Catal. 75 (1982) 78.
- [38] R.J. Madix, Adv. Catal. 29 (1980) 1.
- [39] F. Solymosi, J. Kiss, I. Kovács, Surf. Sci. 192 (1987) 47.
- [40] M.A. Barteau, Catal. Lett. 8 (1991) 175.
- [41] A. Boddien, F. Gärtner, R. Jackstell, H. Junge, A. Spannenberg, W. Baumann, R. Ludwig, M. Beller, Angew. Chem. Int. Ed. 49 (2010) 8993.
- [42] C. Fellay, P.J. Dyson, G. Laurenczy, Angew. Chem. Int. Ed. 47 (2008) 3966.
- [43] S. Enthaler, ChemSusChem 1 (2008) 801, and references therein.
- [44] S. Enthaler, J. von Langermann, T. Schmidt, Energy Environ. Sci. 3 (2010) 1207, and references therein.
- [45] F. Solymosi, R. Barthos, A. Kecskeméti, Appl. Catal. A Gen. 350 (2008) 30, and references therein.
- [46] R.C. Weast, M.J. Astle (Eds.), CRC Handbook of Chemistry and Physics, 64th ed., CRC Press, 1983.
- [47] R.E. Eischens, W.A. Pliskin, in: Actes Congr. Intern. Catalyse 2e Paris, 1961, p. 789.
- [48] W.M.H. Sachtler, J. Fahrenfort, Actes du Deuxieme Congres Internationale de Catalyse (1961) 831.
- [49] F. Solymosi, É. Novák, A. Molnár, J. Phys. Chem. 94 (1990) 7250.
- [50] A. Berkó, G. Ménesi, F. Solymosi, J. Phys. Chem. 100 (1996) 17732, and references therein.
- [51] M. Mavrikakis, M.A. Barteau, J. Mol. Catal. A Chem. 131 (1998) 135.
- [52] Y.B. Jang, T.H. Kim, M.H. Sun, J. Lee, S.J. Cho, Catal. Today 146 (2009) 196.